

Frustration and disorder in granular superconductors

W. Y. Shih, C. Ebner, and D. Stroud

Department of Physics, The Ohio State University, Columbus, Ohio 43210

(Received 17 January 1984)

We consider the behavior of ordered and disordered three-dimensional weakly coupled arrays of superconducting grains embedded in a nonsuperconducting host and placed in a magnetic field B . In ordered simple-cubic arrays, with \vec{B} parallel to a crystal axis and nearest-neighbor interactions, both Monte Carlo and molecular-field calculations show that T_c is periodic in B with a period of one flux quantum per unit square perpendicular to the field, and with complex substructure, as found previously in two-dimensional ordered arrays. The dependence of T_c upon \vec{B} is also shown to be highly anisotropic. Positionally disordered arrays are shown to behave at sufficiently strong fields very much like a spin-glass: They are, in fact, a physical realization of the "gauge glass" discussed by several authors. Varying the magnetic field, at strong fields, is equivalent to jumping from one "spin-glass replica" to another. Monte Carlo calculations for a model of dilute Pb spheres in a Zn host show a continuous transformation from an "xy ferromagnet" to spin-glass behavior: $T_c(B)$ first drops with increasing field, then saturates at strong fields. For weaker disorder, $T_c(B)$ is predicted to be a damped oscillating function of B . Both ordered and disordered samples are predicted to be anisotropic superfluids in a magnetic field. The implications of these predictions for measurements of kinetic inductance and other transport properties are briefly discussed.

I. INTRODUCTION

Among the most novel of superconducting materials are those composed of small grains of superconductor embedded in a nonsuperconducting host.¹ The latter can be any of a variety of substances: insulator, semiconductor, normal metal, or superconductor with a lower transition temperature. The superconducting particles can vary in size from 100 Å to microns in diameter, and can be spherical or irregular in shape, depending on how the composite is made. A particularly striking feature of such materials is the existence of two superconducting transitions: a higher one near the transition temperature T_{c0} of the superconducting grains, at which the grains become superconducting but the matrix remains normal; and a lower transition at a temperature T_c where the composite as a whole becomes perfectly conducting at sufficiently low current densities. The latter transition is due to the onset of weak coupling between the superconducting grains through the normal matrix—Josephson coupling, if the matrix is an insulator and proximity-effect coupling for a normal-metal host. While this double transition is believed to occur in a number of materials, particularly strong evidence is provided by specially prepared ordered two-dimensional arrays of superconducting grains: Above T_c one finds an oscillatory magnetoresistance with a period of one flux quantum per unit cell of the grain lattice.^{2,3} It is difficult to account for this behavior in any other way than the onset of a phase transition due to weak coupling, as modulated by a magnetic field. The details of the transition are not yet fully understood, but its origin as a phase-coherent phenomenon arising from weak coupling is generally agreed upon.

The purpose of this paper is to discuss the behavior of weakly coupled granular superconductors, of the kind just

described, in a magnetic field. The discussion will be limited to "three-dimensional" materials, that is, to composites in which all relevant length scales are small in comparison to all three dimensions of the sample. Thus, in particular, the composite is many times thicker than the average spacing between superconducting grains. Composites only one layer thick can be prepared in characterized form, and exhibit special phenomena of great interest such as the vortex-unbinding transition described by Kosterlitz and Thouless,²⁻⁷ but will not be considered here.

The model we use to describe this behavior is a pseudospin picture which has been used by various authors⁸⁻¹³ to describe other properties of granular superconductors. According to this picture, each superconducting grain acquires a gap, or order parameter, as the temperature is lowered below the single-grain transition temperature T_{c0} . The amplitude of this gap is fixed by the characteristics of the single grain, but its phase is not, in the absence of intergrain coupling. The gap thus behaves as a two-component ("x-y") spin. The weak coupling between grains (proximity or Josephson) acts as a ferromagnetic interaction between the "spins" in the absence of an applied magnetic field. The lower transition at T_c , in this picture, is thus a phase-coherent transition in which the phases of the gap acquire long-range order. The introduction of a magnetic field, as is well known, strongly affects superconductive weak coupling. In the present case, its effect is to introduce "frustration"¹⁴ into the coupling, so that some couplings are ferromagnetic while others tend to align spins at an angle other than zero degrees. The existence of frustration means that there is no ordered state of the phases which can simultaneously minimize the energies of all the weak "bonds." Increasing the field serves to vary this frustration continuously so that at sufficiently high fields a disordered sam-

ple of granular superconductor will behave very much like a spin glass rather than a ferromagnet.

The expected behavior of the superconducting composite can now be deduced from the known properties of the pseudospin model. Since the Hamiltonian describing the weak coupling between superconducting grains is periodic in magnetic field, with a period of one flux quantum per unit cell of the grain lattice, given nearest-neighbor interactions, it follows that all measurable properties of an ordered array (such as transition temperature T_c , critical current, and resistivity above T_c) will be similarly periodic. On the other hand, a disordered array will have couplings very similar to those found in a spin glass at sufficiently strong magnetic fields; one thus expects that T_c will decrease from its zero-field, "ferromagnetic" value to a lower "spin-glass" value at large magnetic field, the latter remaining unchanged as B is further increased. These expectations are all confirmed by detailed calculations, as described later in this paper.

The present point of view differs somewhat from that of a recent body of work,¹⁵⁻¹⁹ beginning with de Gennes, on the behavior of composite superconductors in a magnetic field. This latter work has not addressed the question of weak-coupled superconductors, but instead considers arrangements of thin superconducting wires linked by magnetic flux. The emphasis of this work has been on low fields and on the behavior of these networks near a connectivity or percolation threshold. The network problem proves to be closely related to the solution of the Schrödinger equation on a similar network in the presence of a magnetic field. This same equation plays a role in the present problem also, as explained below. Thus, the two problems are clearly related, though not identical.

We now turn to the body of the paper. In Sec. II we describe the model to be analyzed, and give a qualitative discussion of the behavior to be expected from it. Results for ordered and disordered three-dimensional arrays are presented in Secs. III and IV. The possible connection between our results and experiment are then discussed in Sec. V

II. THE MODEL AND ITS QUALITATIVE BEHAVIOR

We consider a material with N grains in volume V , the i th grain centered at \vec{x}_i and having a complex energy gap $\psi_i = \Delta_i \exp(i\phi_i)$. The grains are weakly coupled via the nonsuperconducting host; in the absence of a magnetic field the coupling energy between grains i and j is

$$E_{ij} = -J_{ij} \cos(\phi_i - \phi_j), \quad (2.1)$$

where the exact form of J_{ij} depends on the medium through which the coupling occurs. If the medium is an insulator, the coupling is via the Josephson effect and

$$J_{ij} = \frac{h}{2e} I_{ij} \quad (2.2)$$

with²⁰

$$I_{ij} = \frac{\pi}{2} \frac{\Delta(T)}{eR_{ij}} \tanh \left[\frac{\Delta(T)}{2k_B T} \right] \quad (2.3)$$

for a junction between two identical grains each having the same gap $\Delta(T)$. In (2.3) R_{ij} is the resistance between grains i and j in their normal state, and T is the absolute temperature. On the other hand, if the coupling is through a normal metal via the proximity effect, Eq. (2.2) is replaced by¹⁰

$$J_{ij} = C(1 - T/T_{cs})^2 \exp[-r_{ij}/\xi_n(T)], \quad (2.4)$$

where C is a constant, T_{cs} is the transition temperature of the superconducting grains, $r_{ij} = |\vec{x}_i - \vec{x}_j|$ is the separation between grains, and $\xi_n(T)$ is the coherence length of the normal metal.

The Hamiltonian describing the entire array of grains is in both cases

$$H = - \sum_{\langle ij \rangle} J_{ij} \cos(\phi_i - \phi_j), \quad (2.5)$$

where the sum runs over all distinct pairs of grains. The thermodynamics of the model are obtained from the classical partition function

$$Z = \int (\pi d\phi_i) \exp(-H/k_B T), \quad (2.6)$$

which shows that the behavior of the system is isomorphic to a classical planar or x - y model with temperature-dependent coupling constants.

In the presence of a static external magnetic field B , the behavior of the array is changed dramatically. The Hamiltonian describing the array is now expressed as

$$H = - \sum_{\langle ij \rangle} J_{ij} \cos(\phi_i - \phi_j - A_{ij}) \quad (2.7)$$

with

$$A_{ij} = \frac{2\pi}{\Phi_0} \int_i^{j \rightarrow} \vec{A} \cdot d\vec{l}. \quad (2.8)$$

In (2.8) $\Phi_0 = hc/2e$ is an elementary flux quantum, and it is understood that the line integral is taken along the path directly joining the centers of grains i and j . Equations (2.7) and (2.8) involve, of course, a number of approximations. For example, the possibility that J_{ij} might depend on B as well as T is suppressed. In addition, if the grains are large compared with the grain penetration depth, flux will be expelled from the grains and the local field B will not be identical to the applied field. The same is true if the penetration depth of the composite is *not* large compared with an intergrain separation. Finally, if the junctions are wide, the integral in (2.8) must be replaced by a suitable average of A_{ij} over the junction width. The present model thus represents a considerable idealization of a real composite, but its behavior is nonetheless sufficiently interesting to consider it in detail.

In order to make rough estimates of the behavior of this model, we assume, for convenience, a magnetic field in the z direction, $\vec{B} = B\hat{z}$, and use the gauge $\vec{A} = Bx\hat{y}$. (The partition function is, of course, gauge invariant.) The phase factor A_{ij} then takes the form

$$A_{ij} = (2\pi/\Phi_0) Bx_{ij}(y_j - y_i), \quad (2.9)$$

where $x_{ij} = (x_i + x_j)/2$ is the average x coordinate along the bond joining grains i and j . Consider first the case

where the grains are arranged on a simple-cubic lattice of lattice constant d , with axes parallel to x , y , and z . From Eq. (2.9) with nearest-neighbor interactions only, the Hamiltonian (2.7) is periodic in B with a period of one flux quantum per unit cell. Thus the transition temperature $T_c(B)$ at which the Hamiltonian (2.7) undergoes a phase transition will also be periodic in B with the same period. The characteristic field describing this periodicity will be of the order of 1 G for a lattice constant d of order microns and 10^4 – 10^5 G for very small grains on a lattice with a lattice constant of order 100 Å.

If B is not parallel to one of the axes of the grain lattice, there will be three periods in the problem, corresponding to one flux quantum per unit square perpendicular to each of the axes. These may be mutually commensurate or incommensurate. The corresponding $T_c(B)$ is then expected to show, in general, very complex behavior, reflecting all three periods as well as much substructure.

Next we consider a disordered system described by the Hamiltonian (2.7). Here it is clearly important to distinguish between “compositional” and “positional” disorder. Compositional disorder is exemplified by a site-diluted simple-cubic lattice of superconducting grains with nearest-neighbor interactions. In this case, the Hamiltonian remains periodic with a period of one flux quantum per d^2 , and all the thermodynamic properties of this system are also periodic with this period. In the more realistic case of positional or “amorphous” disorder, the grains do not occupy the sites of a lattice and the Hamiltonian has no periodicity in \vec{B} . The behavior here is expected to be more complex. At zero field, the composite will behave as a disordered ferromagnet, since all the x - y spins are coupled ferromagnetically. At sufficiently strong fields, however, nearly all the phase factors A_{ij} will be large compared to 2π . (The only exceptions, in the gauge being considered, are bonds precisely oriented in the xz plane.) Thus the couplings J_{ij} will tend to orient the phases at essentially random angles, and the composite will behave very much like a spin glass. It is, in fact, a physical realization of the “gauge glass” mentioned by several authors.²¹ Once the “high-field limit” has been attained, further increases in the field are not expected to alter the thermodynamic properties, since the interactions are already randomized. (However, varying the magnetic field in this regime is equivalent to jumping from one spin-glass replica to another.) Thus the phase-ordering transition temperature should decrease from its zero-field value, as the field is increased, ultimately saturating at a lower, spin-glass value. The crossover field dividing low-field from high-field behavior should be of order one flux quantum per d^2 , where d is now a typical nonzero bond-length.

A schematic of the two types of behavior just described is shown in Fig. 1. Also shown is a sketch of an intermediate-case, “weak” amorphous disorder. In this case all closed loops of nonzero bonds have projected areas perpendicular to \vec{B} which are nearly multiples of the same fundamental area. Thus, fields which are harmonics of the same field (one flux quantum per fundamental area) will correspond to Hamiltonians which are nearly ferromagnetic, such as the zero-field case. One thus expects

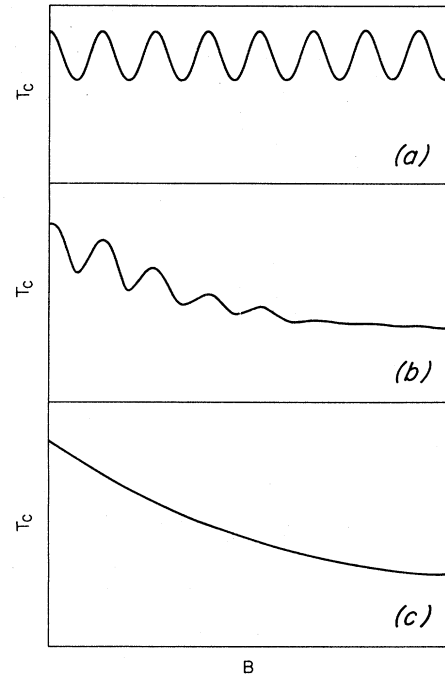


FIG. 1. Schematic of the phase diagram expected for a three-dimensional composite in the presence of a magnetic field. (a) Ordered simple-cubic lattice field parallel to one of the principal axes: phase-transition temperature $T_c(B)$ is periodic in B with a period of one flux quantum per unit square and complex substructure. (b) Weak disorder: $T_c(B)$ has damped oscillations and saturates at a value lower than $T_c(0)$. Strong-field limit is spin-glass-like. (c) Strong disorder: $T_c(B)$ decreases monotonically from a zero-field “disordered ferromagnet” behavior to the strong-field spin-glass regime. Not shown: ordered simple-cubic lattice with \vec{B} not along a crystal axis. $T_c(B)$ is expected to oscillate with three possibly incommensurate periods and complex substructure.

a phase boundary which has damped oscillations, as shown, approaching a saturation spin-glass value at high fields.

Note that the region shown as “phase ordered” in the figure has different meanings in the ferromagnetic and spin-glass regimes. In the ferromagnetic region, the phases are lined up parallel, whereas in the spin-glass limit they are probably frozen in more or less random orientations. All the usual uncertainties that prevail in theories of ordering in more conventional spin glasses²² are present in this model also, as discussed in subsequent sections, but we will provide numerical evidence that the phase diagram shown in Fig. 1 is substantially correct.

III. ORDERED ARRAYS

In order to verify the qualitative predictions of the preceding section, we have investigated the behavior of the Hamiltonian (2.7) for both ordered and disordered arrays, using Monte Carlo techniques.²³ The analysis for ordered lattices was carried out for simple-cubic arrays with

nearest-neighbor interactions only; to further clarify the analysis, the coupling constants were assumed to be temperature independent. The model (2.7) is then equivalent, in the language of statistical mechanics, to an x - y Hamiltonian with a continuously varying frustration $\vec{f}=(f_x, f_y, f_z)$; the i th component of frustration is the flux in excess of an integer number of the flux quanta

$$\langle O \rangle = \frac{\int O(\phi_1, \dots, \phi_N) \exp[-H(\phi_1, \dots, \phi_N)/k_B T] \prod_{i=1}^N d\phi_i}{Z}, \quad (3.1)$$

where $O(\phi_1, \dots, \phi_N)$ is some operator dependent on the N phases. Calculations were performed on cells ranging from $4 \times 4 \times 4$ to $16 \times 16 \times 10$ with periodic boundary conditions, with the use of the standard Metropolis algorithm.²⁴ Typically, 10 000 to 20 000 passes were made through the entire lattice after the first 3000 to 5000 were thrown out. The data points shown are the results of averaging three to six independent runs.

While this procedure permits any time-independent equilibrium quantity to be computed, we have concentrated on three averages of particular interest: the specific heat C_v , the Edwards-Anderson (EA) order parameter η , and the helicity modulus tensor $\vec{\gamma}$. C_v is readily computed from its fluctuation expression

$$C_v = [\langle H^2 \rangle - \langle H \rangle^2] / (Nk_B T^2) \quad (3.2)$$

for any size of lattice. While C_v as defined by (3.2) is certainly of interest in determining whether or not a phase transition occurs, any anomaly is likely to be difficult to see in a real superconducting composite, since the phase degrees of freedom described by (3.2) are very few in number (one per grain) compared to those associated with gap amplitude. The EA order parameter²⁵ is defined by

$$\eta = N^{-1} \sum_{i=1}^N |\langle e^{i\phi_i} \rangle|, \quad (3.3)$$

$$\gamma_{xx} = N^{-1} \left[\sum_{\langle ij \rangle} J_{ij} x_{ij}^2 \langle \cos(\phi_i - \phi_j - A_{ij}) \rangle - \frac{1}{k_B T} \left\langle \left(\sum_{\langle ij \rangle} J_{ij} x_{ij} \sin(\phi_i - \phi_j - A_{ij}) \right)^2 \right\rangle + \frac{1}{k_B T} \left\langle \sum_{\langle ij \rangle} J_{ij} x_{ij} \sin(\phi_i - \phi_j - A_{ij}) \right\rangle^2 \right], \quad (3.6)$$

where $x_{ij} = x_j - x_i$; analogous expressions hold for other components of $\vec{\gamma}$.

Some of our results for ordered simple-cubic arrays are shown in Figs. 2–4 for a variety of field strengths. The results clearly indicate that a phase transition does occur for all the fields investigated, and that T_c is strongly dependent on both the direction and the magnitude of the field. No severe difficulty was encountered in obtaining convergence, even for systems with relatively large unit cells. The peak in the C_v increases with increasing Monte Carlo cell size, as expected for a system in which a phase transition occurs, but we have not considered cells which are sufficiently large to apply finite-size scaling and ob-

tain an exponent describing the behavior of C_v near $T_c(f)$. (Similar behavior is seen in the specific-heat peak for other values of f , though the size dependence is more difficult to observe.) Several components of the helicity modulus fall sharply at $T_c(f)$, and there is a nonzero tail at higher temperatures due to finite-size effects. The EA order parameter (not shown) also decreases sharply at T_c but its behavior near the transition is less conspicuous than that of the helicity modulus.

The Monte Carlo analysis was carried out by calculating averages within the canonical ensemble of the form

and is a measure of the degree to which the phases are “frozen” into a particular orientation. It is defined so as to equal unity at $T=0$. As a rule, however, η is found not to be very stable numerically, since the entire array of frozen spins in a (finite) Monte Carlo sample tend to rotate slowly as a block. A more reliable indicator of long-range phase coherence is $\vec{\gamma}$, which measures the cost in free energy of imposing a twist in the phase at the boundaries of the sample.²⁶ The principal elements of $\vec{\gamma}$ are essentially stiffness constants. Rather than imposing a twisted boundary condition and calculating the free energy with the Hamiltonian (2.7), it is more convenient to use periodic boundary conditions and add a term to the Hamiltonian which is equivalent to a twist, as discussed elsewhere.¹¹ The result is

$$\gamma_{ij} = \left[\frac{\partial^2 F}{\partial A'_i \partial A'_j} \right]_{\vec{A}' = \vec{0}}, \quad (3.4)$$

where \vec{A}' represents an added (i.e., in addition to $Bx\hat{y}$) uniform vector potential. Using the definition

$$F = -k_B T \ln Z \quad (3.5)$$

for the free energy, one can easily evaluate the second derivative explicitly for an ordered or a disordered sample, and obtain the following expression for, e.g., γ_{xx} :

tain an exponent describing the behavior of C_v near $T_c(f)$. (Similar behavior is seen in the specific-heat peak for other values of f , though the size dependence is more difficult to observe.) Several components of the helicity modulus fall sharply at $T_c(f)$, and there is a nonzero tail at higher temperatures due to finite-size effects. The EA order parameter (not shown) also decreases sharply at T_c but its behavior near the transition is less conspicuous than that of the helicity modulus.

The behavior exhibited by C_v in three dimensions appears to differ substantially from that seen in the two-dimensional (2D) simulations.⁸ All of our three-dimensional (3D) calculations, at $f = \frac{1}{2}$ and at $f = 1/q$

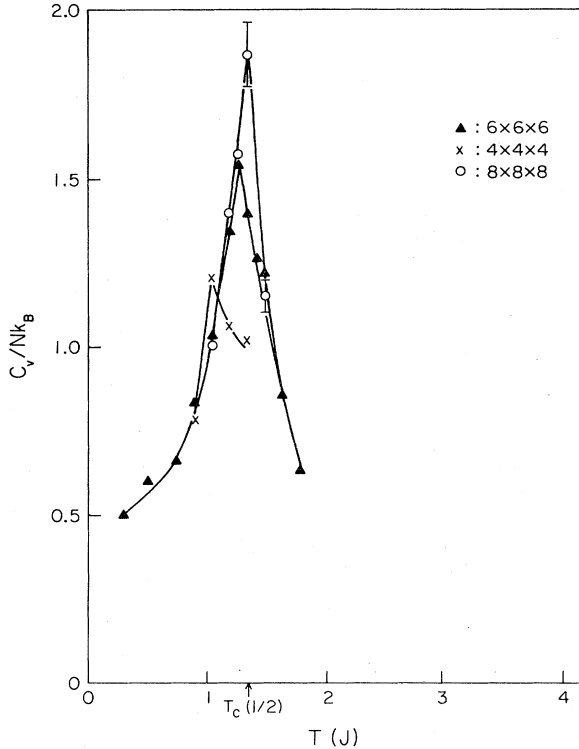


FIG. 2. Specific heat for an ordered simple-cubic lattice (as a function of temperature T in units of J/k_B) with nearest-neighbor interactions J and a field $\vec{f}=(0,0,\frac{1}{2})$ in units of one flux quantum per unit square, as calculated by MC simulation. Numbers denote different MC cell sizes. Arrow denotes estimated infinite-cell transition temperature.

with larger values of q (not displayed in the figures), show a behavior of C_v consistent with a power-law singularity at a critical temperature. Our Monte Carlo (MC) cells are, as indicated above, much too small to provide fully convincing evidence that there is such a singularity, but the results for $f=\frac{1}{2}$ are at least suggestive. By contrast, analogous MC calculations for $d=2$ suggest a power-law singularity only at $f=\frac{1}{2}$.⁸ This behavior has been interpreted as indicating an Ising-type transition at $f=\frac{1}{2}$, with a diverging correlation length of Ising-type domains, but a Kosterlitz-Thouless-type transition at other values of f (with a correlation length not diverging as a power law in $T-T_c$). Our 3D data, therefore, seem to suggest that the transition at *all* values of f is of Ising-type or at least not of Kosterlitz-Thouless type. This would come as no surprise since the Kosterlitz-Thouless transition is a uniquely two-dimensional phenomenon. But more work (both numerical and analytical) is certainly still needed to determine the precise nature and universality class of the 3D transition at various values of f .

It is of interest to compare the values of $T_c(\vec{f})$ as obtained from Monte Carlo simulation with those obtained from mean-field theory. The appropriate mean-field theory was derived by Shih and Stroud;⁹ the mean-field transition temperature proves to map onto the highest-

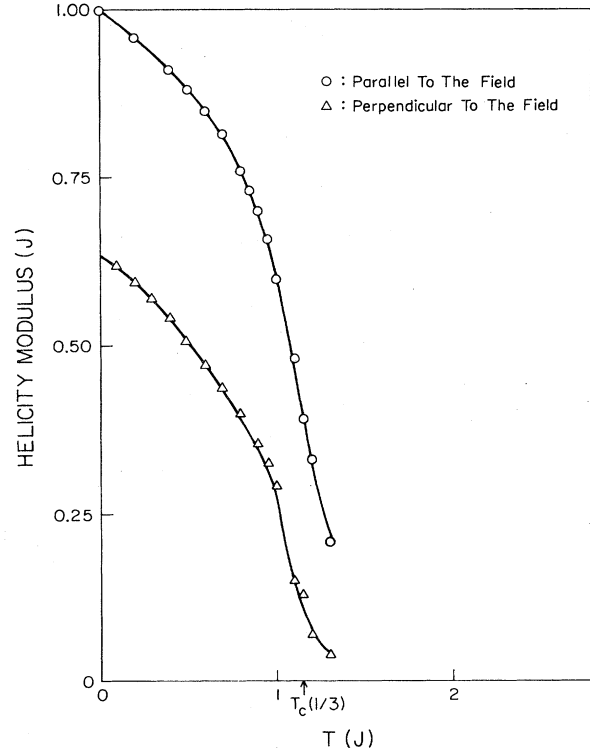


FIG. 3. Longitudinal and transverse components of the helicity modulus $\gamma_{||}\equiv\gamma_{zz}$ and $\gamma_{\perp}\equiv\gamma_{xx}$ for $\vec{f}=(0,0,\frac{1}{3})$ for ordered lattices, as calculated by Monte Carlo simulation. Arrow and horizontal axis as in Fig. 2. The vertical axis denotes the helicity modulus in units of J .

energy eigenvalue of an electron in a tight-binding band in the presence of a magnetic field—a problem considered by Hofstadter.²⁷ The comparison is presented in Figs. 5 and 6. For fields parallel to the z axis, the mean-field transition temperature correctly reproduces some of the qualitative features of the exact numerical results. In particular, $T_c(\frac{1}{3},0,0)$ is found to be lower than $T_c(\frac{1}{2},0,0)$ in both mean-field theory and Monte Carlo calculations. In general, however, the Monte Carlo transition temperatures are substantially lower than the mean field, as is usual in problems of this sort. Note that, in general, the Monte Carlo results (and mean-field theory) are consistent with values of $T_c(\vec{f})$ which are highly sensitive to both the magnitude and the direction of \vec{f} .

An interesting feature of the results is that $\vec{\gamma}$ is not, in general, a multiple of the unit tensor. Thus, the phase-ordered state corresponds to an *anisotropic superfluid*. The physical reason for this is particularly obvious if one considers a field parallel to one of the crystal axes, for example, the z axis. In this case it is clearly more difficult to impose a twist with an axis parallel to z , than a twist in the x - y plane (the former requires twisting bonds which are all ferromagnetically aligned), and this is reflected in the behavior of $\vec{\gamma}$ as shown in Fig. 2. For $\vec{f}=(f,0,0)$ and $f=\frac{1}{5}$ and $\frac{1}{4}$ (not shown), we see evidence of *much greater*

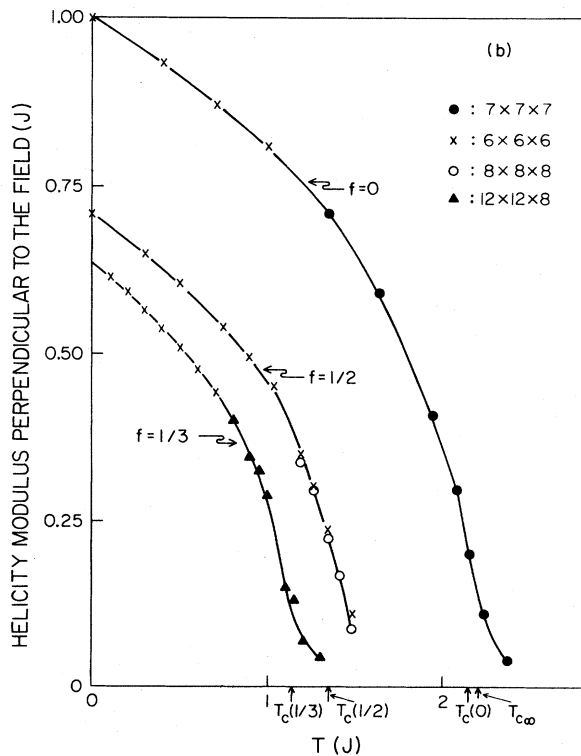
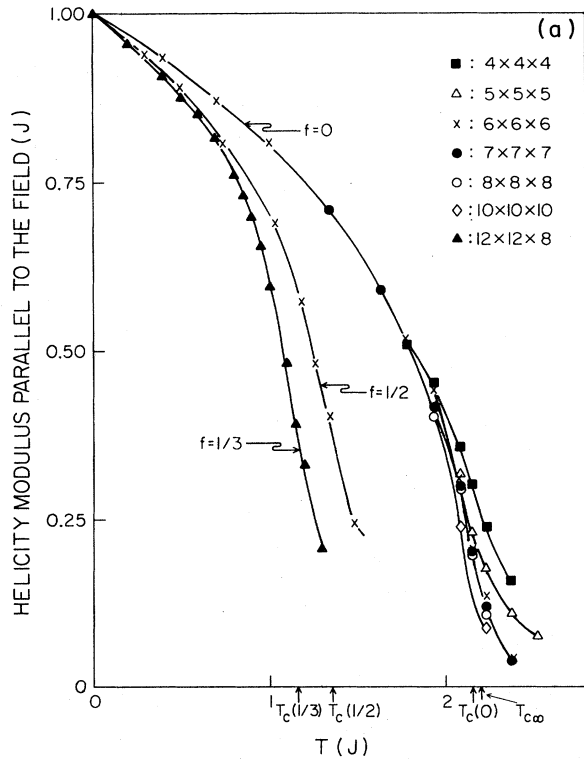


FIG. 4. (a) Longitudinal and (b) transverse components of the helicity modulus for ordered lattices at several values of field, as calculated by Monte Carlo simulation. Axes and arrows as in Fig. 3. $T_{c\infty}$ denotes the true transition temperature of the third x - y model as derived from series expansions [M. Ferer, M. A. Moore, and M. Wortis, Phys. Rev. B **8**, 5205 (1973)].

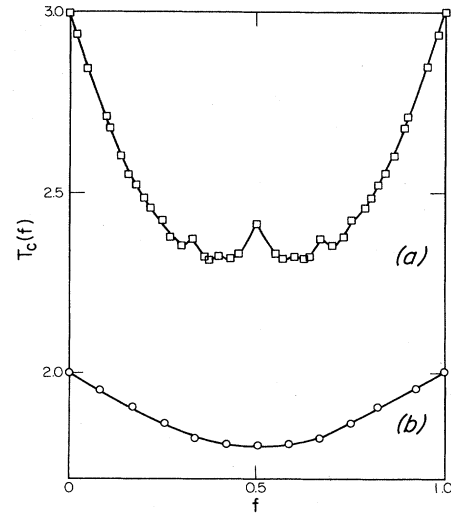


FIG. 5. Transition temperature $T_c(f)$ as a function of $\vec{f}=(0,0,f)$ for (a) an ordered simple-cubic lattice of grains, and (b) a site-diluted simple-cubic lattice of grains with nearest-neighbor couplings and a site occupancy of $p=0.4896$. In the disordered case, the lattice is $(12 \times 12 \times 12)$, while in the ordered case the lattices were $[(M/f) \times (M/f) \times (M/f)]$ with $M \geq 1$. The calculations were carried out by the molecular-field theory of Ref. 9.

anisotropy in $\vec{\gamma}$ near $T_c(\vec{f})$ than for $f = \frac{1}{2}$ and $\frac{1}{3}$. The two components may possibly vanish with a different power-law behavior near T_c . Experimentally, an anisotropic superfluid might be probed by measurements of the kinetic inductance, i.e., the imaginary part of the conductivity, as discussed in Sec. V.

As a simple estimate of the effects of compositional

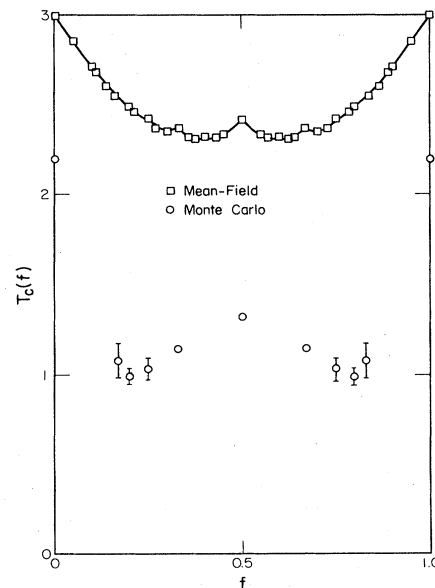


FIG. 6. Transition temperature $T_c(f)$ in units of J/k_B for $\vec{f}=(0,0,f)$ and a simple-cubic lattice. Both mean-field and Monte Carlo results are shown. The line is merely a guide to the eye.

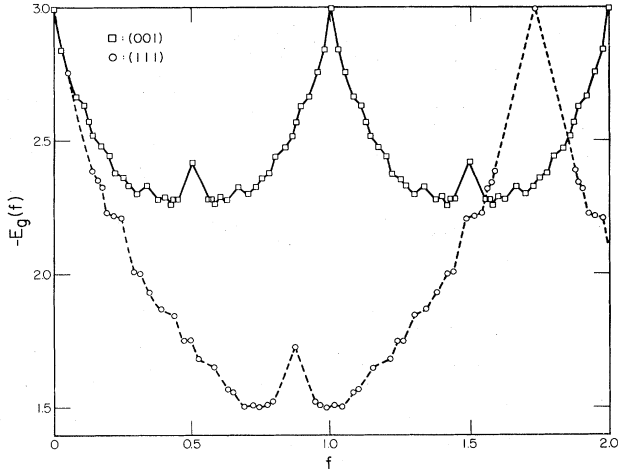


FIG. 7. Ground-state energy $-E_g(f)$ in units of J for \vec{f} parallel to [001] and to the [111] axes, plotted as a function of $|\vec{f}|=f$. Once again the results are for a fully occupied simple-cubic lattice; the lines are a guide to the eye.

disorder, we have considered a site-diluted simple-cubic lattice of spheres with nearest-neighbor coupling in the presence of an applied field parallel to the z axis, using the mean-field theory of Ref. 9. The mean-field transition temperature in this case maps onto the highest-energy eigenvalue of an electron in a *site-diluted* tight-binding bond in the presence of a magnetic field. We have solved the relevant equations numerically and plotted the resulting transition temperature in Fig. 5. The extensive structure of the ordered case is largely washed out: $T_c(B)$ seems, in fact, to fall off and then saturate at sufficiently strong B , very much like the schematic of Fig. 1(c). Further confirmation of this behavior will be found in the Monte Carlo simulations of the next section.

Figure 7 shows the ground-state energy E_g , which is another measure of the anisotropy shown in Figs. 2–4. The energy $-E_g$ may be calculated exactly from the mean-field theory of Ref. 9 if the self-consistency equations are iterated to convergence as described in that reference; E_g is shown as a function of field strength for fields in the [100] and [111] directions. Note the apparently nonanalytic variation of E_g with B in both cases—a feature previously found in the two-dimensional results as well. The strong anisotropy mentioned above is evident in the difference between the two curves.

IV. DISORDERED THREE-DIMENSIONAL ARRAYS

We turn next to the more easily realized situation of *disordered* arrays of superconducting particles embedded in a nonsuperconducting host. In order to simulate as closely as possible a real material, we have tried to model our system after a composite of identical Pb grains embedded in a Zn host, a material studied by Boysel *et al.* in the zero-field limit.²⁸ The grains are then assumed to be coupled by a proximity interaction of the form (2.4), with the normal-metal coherence length $\xi_n(T)$ given by the usual Ginzburg-Landau expression. Thus the model sys-

TABLE I. Parameters entering into model PbZn calculation as described in the text.

Transition temperature of Pb ($T_{c,Pb}$)	7.2 K
Transition temperature of Zn ($T_{c,n}$)	0.8 K
Radius of Pb squares	1.0 μm
Volume fraction of Pb spheres	0.5%
Zero-temperature coherence length of Zn (ξ_0)	30000 \AA
Coupling constant C [Eq. (2.4)]	720 K
Magnetic field scale unit (Figs. 9–14)	0.156 G

tem is described by a Hamiltonian given by Eqs. (2.7), (2.8), and (2.4) with

$$\xi_n = \xi_0 \left(\frac{T - T_{cn}}{T_{cn}} \right)^{-1/2} \quad (4.1)$$

The remaining parameters used in the calculation are listed in Table I. The numerical expression for the normal coherence length is appropriate to the dirty limit ($\xi_0 \gg$ mean free path).²⁹

The Monte Carlo simulation was carried out in a model unit cell with 300 to 500 particles, having periodic boundary conditions, and a packing fraction (volume fraction occupied by the Pb spheres) of 0.5%. All particles were assumed to be equal in size. In order to generate the amorphous structure, the unit cell was divided into an $N \times N \times N$ grid with N^3 total points. To this lattice spheres were added at random. The placing of spheres on a lattice is of course an artifact which makes our model system differ from a real composite with amorphous disorder, but for a sufficiently fine grid and sufficiently dilute arrangement of spheres, the effects of this artifact should be small. The lattice is necessary in the simulations to ensure a Hamiltonian with the periodicity of the

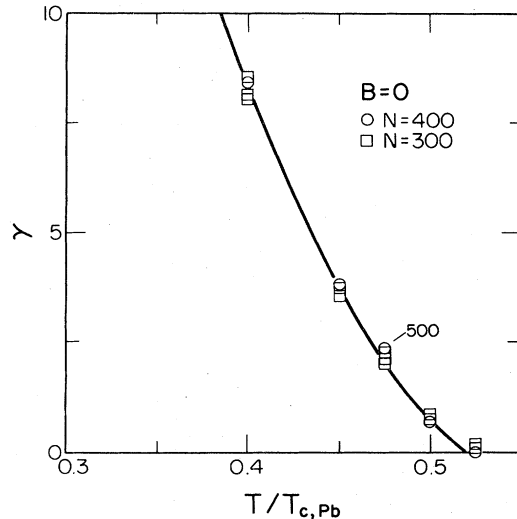


FIG. 8. Calculated helicity moduli $\gamma_{||}=\gamma_{\perp}=\gamma$ for a disordered arrangement of 0.5% 1- μm -radius Pb spheres randomly dispersed in a Zn matrix, as described in the text. Calculations are carried out via Monte Carlo simulations. The applied magnetic field $B=0$. Results are given for several different MC runs and for 300, 400, and 500 particles.

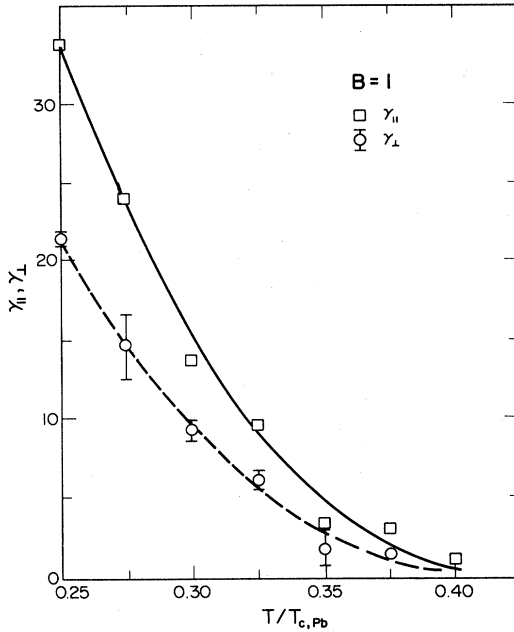


FIG. 9. Same as Fig. 8, but for $B=1$ scale unit corresponding to approximately 0.156 G. For the transverse case, the points shown are the averages of the calculated γ_{xx} and γ_{yy} .

Monte Carlo unit cell. When the magnetic field is chosen to be a multiple of one flux quantum per L^2/N where L is the edge of the unit cell, then the requirement of periodicity is satisfied. The necessity of discretizing both field and lattice thus arises only from practical constraints on the sample size imposed by computer capacity, certainly not because of any fundamental physical requirements. We have used $N=30$ with 300 particles and $N=42$ and 500 particles; in general, N was chosen such that the unit of magnetic field (see Table I) is independent of the num-

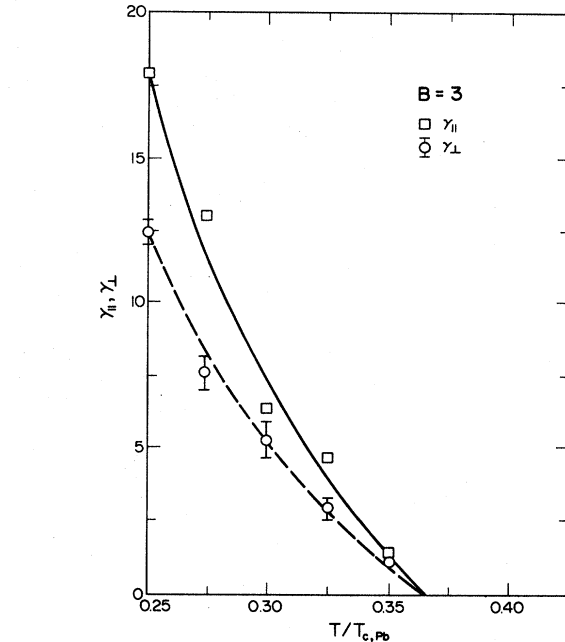


FIG. 11. Same as Fig. 9, but for $B=3$ scale units.

ber of particles and also such that the nearest-neighbor distance in the lattice is slightly larger than the diameter of the Pb spheres.

The one remaining parameter in the model is the overall strength of the coupling constant, J_{ij} . This was chosen so as to generate a phase-ordering transition temperature $T_c(B)$ of about 4 K at $B=0$, consistent with what was found by Boysel *et al.*²⁸ for $\sim 1 \mu\text{m}$ radius. Results for finite field were calculated on the assumption that ξ_0 for Zn is independent of B , a hypothesis that is probably reasonable for the small fields being considered.

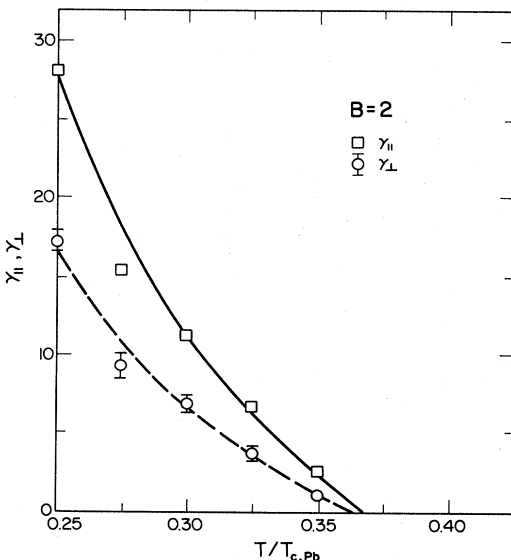


FIG. 10. Same as Fig. 9, but for $B=2$ scale units.

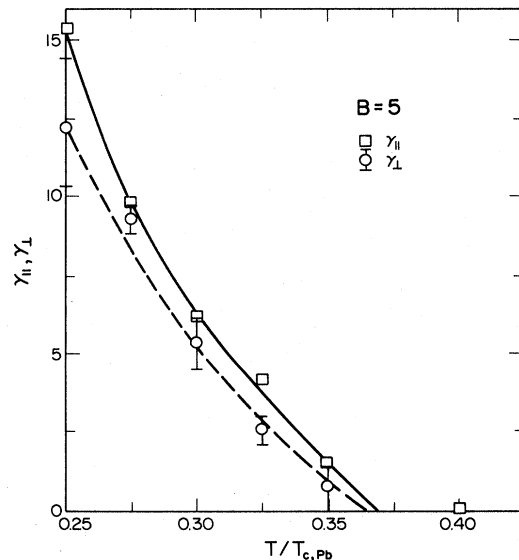


FIG. 12. Same as Fig. 9, but for $B=5.0$ scale units.

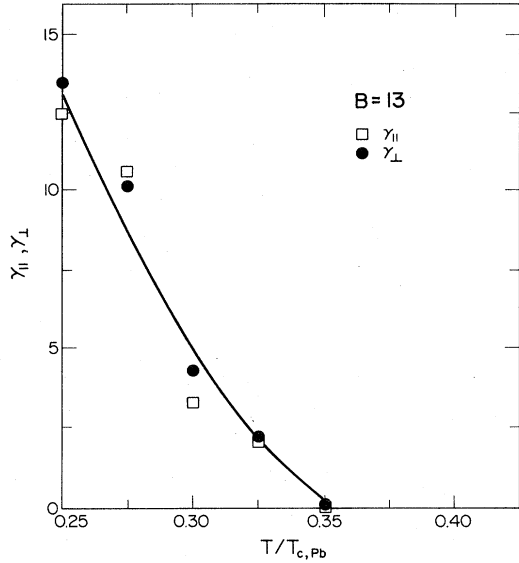


FIG. 13. Same as Fig. 9, but for $B = 23.0$ scale units.

The exponentially decaying constant J_{ij} was cut off at separations greater than eight sphere diameters, which in the worst case (300 particles) was about $0.25L$. At this distance, the coupling strength is typically several orders of magnitude smaller than it is for nearest neighbors. At the packing fraction of 0.5%, any given particle interacts with some 12 to 30 neighbors, 20 being about the mean.

At high fields, convergence of all quantities (specific heat, EA order parameter, and helicity modulus) is much slower than in the ordered case (typically by a factor of at least 10), as is typical of spin-glass-like model systems. It is, of course, impossible to say with absolute certainty that our helicity moduli correspond to true time-independent

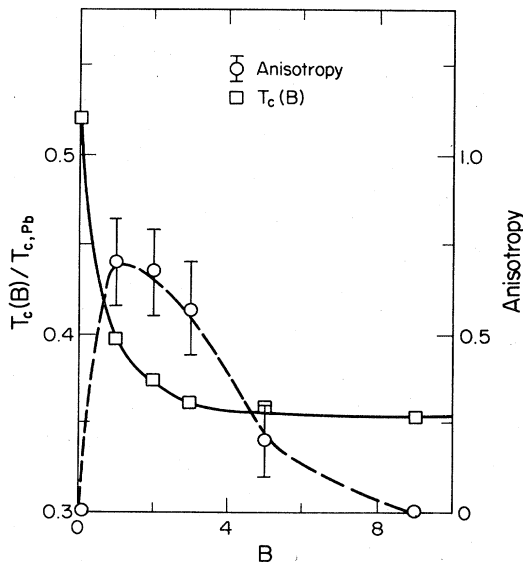


FIG. 14. Squares: transition temperature $T_c(B)$ as deduced from Figs. 8–13. Circles: anisotropy $\gamma_{||}/\gamma_{\perp}-1$ at $T/T_{c,Pb}=0.30$, as deduced from Figs. 8–13.

values, but in the cases shown they appear to have stabilized over a period of 20000 Monte Carlo passes through the sample. The EA order parameter, by contrast, is unstable: its value depends on the number of steps over which it is averaged, because of the tendency for the entire group of spins in the Monte Carlo sample to rotate slowly as a block as mentioned previously.

Figures 8–14 show the helicity moduli, anisotropy, and transition temperatures for the disordered “Pb-Zn” model just described. If the grains are taken to have radii $1 \mu\text{m}$, then the magnetic field scale constant B_0 is 0.156 G at the dilutions we consider; fields much larger than this are in the high-field limit.

The figures clearly indicate support for the qualitative predictions of Sec. II. In particular, $T_c(B)$ falls from its value of 3.7 K at $B=0$ to a value of 2.5 K near $B=B_0$, saturating near this value and changing little for higher fields. The lack of oscillations in $T_c(B)$ is explained by the great variations in projected areas of the closed loops of nonzero coupling strengths through which flux may penetrate. Each loop corresponds to a different natural periodicity, and the system as a whole integrates over these periodicities in the way shown in the figures. The helicity modulus is isotropic again in the high-field limit. The isotropy in this latter case is due to the fact that all the couplings are essentially randomized, provided their direction is not precisely in the x - y plane.

V. DISCUSSION

Many of the predictions of the preceding sections should be subject to straightforward experimental verification. The preparation of an ordered three-dimensional array of weak links would, of course, be very difficult, but if such a material could be designed, it would be expected to have a transition temperature $T_c(B)$ which is an oscillating function of \vec{B} and is highly sensitive to field direction as well as magnitude. Below this transition one expects zero resistance in the limit of weak applied currents. In the more accessible case of disordered three-dimensional arrays, one expects $T_c(B)$ to decrease with increasing field, saturating at a constant value at high fields (i.e., fields that are large compared to one flux quantum per loop of connected weak links). The transition from low-field to high-field behavior is expected to be of the order of 1 G for samples such as those of Ref. 28.

The helicity modulus has a somewhat less obvious experimental interpretation. It appears that γ_{ij} may be equivalent to the “inverse kinetic inductance,” i.e., to the inductive part of the low-frequency conductivity, and thus may be accessible to ac measurement.³⁰ From its definition, γ_{ij} is the second derivative of Helmholtz free energy with respect to vector potential or

$$\gamma_{ij} \propto \left[\frac{\partial J_i}{\partial A_j} \right]_{T,V}, \quad (5.1)$$

where J_i is the i th component of supercurrent density and A_j is the j th component of an applied vector potential in addition to that which generates the magnetic field. If A_j is produced by an applied electric field, then $A_j = icE_j/\omega$

and it follows that γ_{ij} is related to the imaginary part of the ac conductivity $\sigma_{ij}(\omega)$ by

$$\text{Im}\sigma_{ij}(\omega) \propto \frac{\gamma_{ij}}{\omega}. \quad (5.2)$$

The low-frequency ac response of the composite should thus exhibit the features of the helicity modulus described in preceding sections.

The disordered samples of Sec. IV should show many of the typical characteristics of other types of glasses, such as time dependence of supposedly equilibrium quantities and various kinds of hysteresis. Our Monte Carlo calculations of the helicity modulus, for example, equilibrate much more slowly for disordered systems than do those for frustrated ordered samples, and they exhibit no size dependence, unlike the ordered ones. At temperatures below the transition, the Monte Carlo iteration produces, on rare occasions, a block rotation of 10–30 spins as a group, thereby causing an abrupt change in the helicity modulus. Thus the existence of a true phase transition is somewhat doubtful, just as it is in other types of spin-glass ordering. All these slow-relaxation phenomena³¹ could undoubtedly be studied experimentally via low-frequency conductivity and voltage-noise measurements, both above and below the transition; such measurements should be very sensitive to just the type of fluctuations one expects to see in these materials. Above $T_c(B)$, conductivity measurements should be able to detect the anisotropy seen below $T_c(B)$: In particular, the conductivities parallel and perpendicular to the field will differ once the temperature is sufficiently near T_c so that short-range phase ordering becomes important.

In connection with the gauge-glass regime it is of some interest to compare our model with the results obtained by Hertz³² for a somewhat similar gauge model of a spin glass. Hertz's model is a continuum Ginzburg-Landau-Wilson $n=2$ field theory with a random gauge field and thus may or may not be in the same universality class as our discrete Hamiltonian, though many features seem

closely related. Renormalization-group calculations by Hertz indicate that for dimension $d \leq 4$ the frustration parameter characterizing his model exhibits a runaway, implying either a first-order phase transition or no transition at all. Hertz interprets these results in terms of a mean-field theory in which the transition possibly takes place into an ordered phase with many nearly equally favored spin configurations. Our numerical results in Sec. IV appear to confirm this picture: there are, indeed, none of the hallmarks of a second-order phase transition such as a specific-heat singularity. A more detailed examination of our gauge-glass transition, probably going beyond numerical simulation, would be necessary to determine this interpretation, however.

To summarize, we have presented the first theoretical study of the behavior of three-dimensional granular superconductors in a magnetic field. Ordered three-dimensional samples are found to behave very much like the two-dimensional arrays previously investigated by Teitel and Jayaprakash⁸ and by Shih and Stroud,⁹ but with more complications when the field does not lie along a symmetry axis. The disordered case is found to present the possibility of a system which can be transformed from a disordered ferromagnet to a spin glass by continuous variation of an easily controlled external parameter—the magnetic field. Both the experimental and theoretical ramifications of these materials, especially the disordered ones, are likely to be extensive and should be widely investigated.

ACKNOWLEDGMENTS

We are grateful for many valuable conversations with C. Jayaprakash, S. Teitel, D. Bowman, and W. H. Shih. This work was supported in part by the National Science Foundation (NSF) through the Materials Research Laboratory at the Ohio State University, Grant No. DMR-81-19368, and in part through NSF Grant No. DMR-81-14842.

¹For many reviews of recent work, see the articles in *Inhomogeneous Superconductors—1979 (Berkeley Springs, WV)* edited by D. U. Gubser, T. L. Francavilla, A. Wolf, and J. R. Leibowitz (AIP, New York, 1980); or Proceedings of the NATO Advanced Studies Institute on Percolation, Localization and Superconductivity, Les Arcs, France (unpublished).

²D. J. Resnick, J. C. Garland, J. T. Boyd, S. Shoemaker, and R. S. Newrock, *Phys. Rev. Lett.* **47**, 1542 (1981).

³R. A. Webb, R. F. Voss, G. Grinstein, and P. M. Horn, *Phys. Rev. Lett.* **51**, 690 (1983).

⁴J. M. Kosterlitz and D. J. Thouless, *J. Phys. C* **6**, 1181 (1973).

⁵S. Doniach and B. A. Huberman, *Phys. Rev. Lett.* **42**, 1169 (1979); B. A. Huberman and S. Doniach, *ibid.* **43**, 950 (1979).

⁶J. E. Mooij, M. R. Beasley, and T. P. Orlando, *Phys. Rev. Lett.* **42**, 1165 (1979).

⁷B. I. Halperin and D. R. Nelson, *J. Low Temp. Phys.* **36**, 599 (1979).

⁸S. Teitel and C. Jayaprakash, *Phys. Rev. B* **27**, 598 (1983); S. Teitel and C. Jayaprakash, *Phys. Rev. Lett.* **51**, 1999 (1983).

⁹W. Y. Shih and D. Stroud, *Phys. Rev. B* **28**, 6575 (1983).

¹⁰C. Lobb, D. W. Abraham, and M. Tinkham, *Phys. Rev. B* **27**, 150 (1983); M. Tinkham, D. W. Abraham, and C. Lobb, *ibid.* **28**, 6578 (1983).

¹¹C. Ebner and D. Stroud, *Phys. Rev. B* **23**, 6164 (1981); **25**, 5711 (1982); **28**, 5053 (1983). The third of these articles discusses helicity moduli.

¹²G. Deutscher, Y. Imry, and L. Gunther, *Phys. Rev. B* **10**, 4598 (1974), and references cited therein.

¹³J. Rosenblatt, *Rev. Phys. Appl.* **9**, 217 (1974).

¹⁴G. Toulouse, *Commun. Phys.* **2**, 155 (1977).

¹⁵P. G. de Gennes, *C. R. Acad. Sci. Ser. B* **292**, 9 (1981).

¹⁶R. Rammal and J. C. Angles d'Auriac, *J. Phys. C* **16**, 3933 (1983).

¹⁷G. Deutscher, I. Grave, and S. Alexander, *Phys. Rev. Lett.* **48**, 1497 (1983).

¹⁸R. Rammal, G. Toulouse, and T. C. Lubensky, *Phys. Rev. B* **27**, 2820 (1983); *J. Phys. Lett.* **44**, L65 (1983).

¹⁹D. R. Bowman and D. Stroud, *Phys. Rev. Lett.* **52**, 299 (1984).

- ²⁰V. Ambegaokar and A. Baratoff, *Phys. Rev. Lett.* **10**, 486 (1963); **11**, 104(E) (1963).
- ²¹See, for example, E. Fradkin, B. Huberman, and S. H. Shenker, *Phys. Rev. B* **18**, 4789 (1978).
- ²²For a discussion of some recent calculations on models of spin glasses, see, for example, D. D. Ling, D. R. Bowman, and K. Levin, *Phys. Rev. B* **28**, 262 (1983), and references cited therein.
- ²³For a review of such techniques, see the articles in *Monte Carlo Methods in Statistical Physics*, edited by K. Binder (Springer, Heidelberg, 1974).
- ²⁴Metropolis algorithm, see Ref. 23.
- ²⁵S. F. Edwards and P. W. Anderson, *J. Phys. F* **15**, 965 (1975).
- ²⁶T. Ohta and D. Jasnow, *Phys. Rev. B* **20**, 139 (1979).
- ²⁷D. R. Hofstadter, *Phys. Rev. B* **14**, 2239 (1976).
- ²⁸R. M. Boysel, A. D. Caplin, M. N. B. Dalimin, and C. N. Guy, *Phys. Rev. B* **27**, 554 (1983).
- ²⁹For a discussion of this limit, see e.g., M. Tinkham, *Introduction to Superconductivity* (McGraw-Hill, New York, 1975), pp. 67 and 111.
- ³⁰Measurements of the kinetic inductance have been used by A. T. Fiory, A. F. Hebard, and W. I. Glaberson [*Phys. Rev. B* **28**, 5075 (1983)] to study the superfluid density in thin superconducting films in connection with the Kosterlitz-Thouless transition in such films.
- ³¹See, for example, the discussion by P. W. Anderson, in *Ill-Condensed Matter* (North-Holland/World Scientific, Amsterdam, 1978), p. 163.
- ³²J. A. Hertz, *Phys. Rev. A* **18**, 4875 (1978).